Journal of Applied Science, Engineering, Technology and Management
Vol. 02, Issue 02, December 2024 pp. 25 - 28

Synthesis and Characterization of Zn-doped SnO_2 Nanoparticles through Co-Precipitation Technique: A Comprehensive Analysis

Anisha Joseph
[1]*Research Centre in Physics, Mar Athanasius College (Autonomous)*,
Kothamangalam, Kerala, India, 686666.

[2]*Department of Science and Humanities, Federal Institute of Science and Technology*,
Angamaly, Kerala, India, 683577
anishajoseph@fisat.ac.in

S Deepa
. [1]*Research Centre in Physics, Mar Athanasius College (Autonomous)*,
Kothamangalam, Kerala, India, 686666
sdeepa@macollege.in

Abstract— Tin oxide (SnO_2) nanoparticles are of significant interest due to their unique properties and diverse applications. In this study, pristine and Zn-doped SnO_2 nanoparticles (with Zn doping levels of 1.9 wt% and 3.7 wt%) were successfully synthesized using the co-precipitation method, followed by annealing at 500 °C for 5 hours. X-ray diffraction (XRD) analysis confirmed that all samples exhibited a tetragonal cassiterite structure, with crystallite sizes ranging from 22.5 nm to 28.2 nm, consistent with values obtained from the Williamson-Hall (W-H) plot. The nanoparticles demonstrated preferential orientation along the (110), (101), and (211) planes. Scanning Electron Microscopy (SEM) showed that the Zn-doped SnO_2 nanoparticles had a denser microstructure compared to the pristine samples. The energy band gap, as determined by diffuse reflectance spectroscopy, was found to be in the range of 3.10 eV to 3.22 eV. Fourier Transform Infrared (FTIR) spectroscopy revealed characteristic peaks at 459 cm^{-1}, 604 cm^{-1}, 924 cm^{-1}, 1976 cm^{-1}, 2117 cm^{-1}, and 3651 cm^{-1}, corresponding to the vibrations of various functional groups present in the material.

Keywords — Co-Precipitation, Cassiterite Structure, Functional groups.

I. Introduction

Metal oxide nanoparticles exhibit unique properties that differ significantly from their bulk counterparts due to their enhanced physical and chemical characteristics [1]. These enhanced properties have led to their application across various fields, including energy storage, photocatalysis, sensors, and biomedical engineering [2]. Among the various metal oxide nanoparticles, tin oxide (SnO_2) is particularly noteworthy, especially in sensing applications, due to its high sensitivity, selectivity, and rapid response and recovery times [3].

Nanoparticles can be synthesized using a variety of methods, with chemical methods being particularly important as they allow for precise control over particle size, shape, composition, and surface properties. Commonly used chemical synthesis methods include sol-gel, hydrothermal, chemical oxidation, chemical reduction, co-precipitation, and chemical vapor deposition [4]. In the present work, the co-precipitation method was employed for the fabrication of tin oxide (SnO_2) nanoparticles. This method was chosen for its cost-effectiveness, simplicity, and the ability to control the composition and size of the nanoparticles [5].

II. Material and Methods

The co-precipitation method was employed to synthesize pristine and zinc-doped tin oxide (SnO_2) nanoparticles. Initially, 11.28 g of $SnCl_2 \cdot 2H_2O$ (Sigma-Aldrich, 99.99%) was dissolved in 100 ml of double distilled water under constant stirring using a magnetic stirrer. The appropriate weight percentage of zinc chloride ($ZnCl_2$) was then added to the precursor solution to achieve the desired doping concentration. 1 Molar ammonia solution was prepared and added dropwise to the precursor solution at a rate of 5 drops per minute. This addition was conducted under continuous stirring to maintain a stable reaction environment and to ensure the pH of the solution reached 7, at which point precipitation began. The mixture was stirred for 5 hours to allow for complete precipitation. The resulting precipitate was thoroughly washed with double distilled water 4 to 5 times to remove any impurities, followed by filtration. The purified precipitate was then dried in a hot air oven at 70 °C for 4 hours. After drying, the material was ground into a fine powder using an agate mortar. Subsequently, the powder underwent calcination at 500 °C for 5 hours to obtain the final SnO_2 nanoparticles [6]. This procedure was repeated with varying weight percentages of Zinc Chloride to produce different concentrations of Zinc-doped tin oxide nanoparticles [7].

The structural properties of the prepared samples were analyzed using an X-ray diffractometer (Bruker D8 Advance). The X-ray diffraction (XRD) patterns were recorded to identify the crystalline phases present in the samples. The morphology of the samples was examined using

eISSN 2584-0371

Received for review: 20-08-2024
Accepted for publication: 23-09-2024
Published: 30-09-2024

a Scanning Electron Microscope (Jeol 6390 LA). This analysis provided detailed images of the sample surface, enabling the study of particle size and surface texture. The optical properties of the samples were investigated using Diffuse Reflectance Spectroscopy (DRS) with a Perkin Elmer Lambda 365 spectrophotometer. The DRS measurements were carried out over a wavelength range of 200 nm to 1000 nm, providing insights into the optical absorption characteristics of the samples. Fourier Transform Infrared (FTIR) spectroscopy was conducted to determine the compositional properties of the samples by identifying the functional groups present in the samples.

III. Results and Discussions

A. X-ray diffraction Studies

The diffraction pattern of SnO_2 NPs was characterized by using X-Ray diffraction of Bruker D8 diffractometer. Fig. 1 shows the X-Ray diffraction pattern of the prepared samples and it is observed that all the diffraction peaks of pristine and Zn doped SnO_2 nanoparticles are perfectly matched with JCPDS Card No.21 -1250 [8].

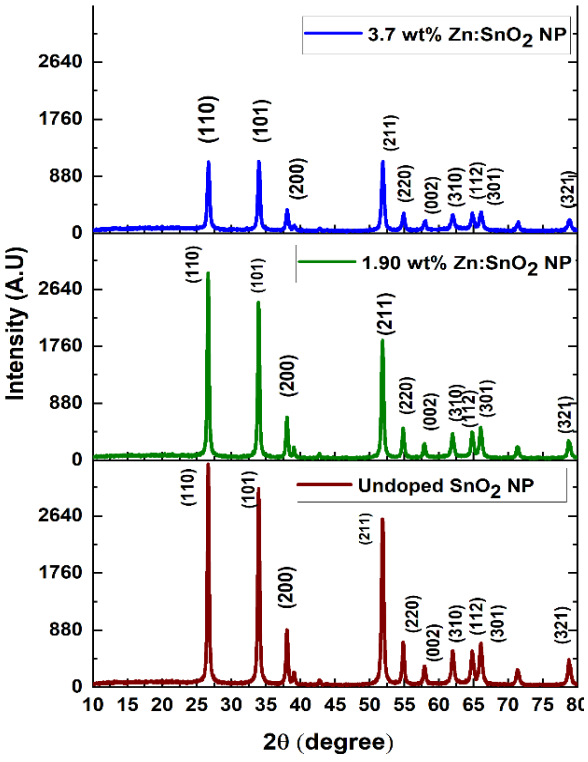

Fig. 1. XRD pattern of the pristine and Zn-doped SnO_2 samples

The intensity of the planes decreases with Zn doping concentration. The crystalline size of the prepared samples is calculated using Debye-Scherrer's equation [9],

$$D = \frac{k\lambda}{\beta Cos\,\theta} \qquad \ldots\ldots\ldots\ldots (1)$$

Where k is a constant with value 0.9,

λ is the wavelength of incident X-Ray beam,

β is the full width half maximum and

θ is the Bragg angle.

The crystalline size is also calculated using Williamson-Hall plot and is in well aligned with that of the value calculated from XRD data [10].

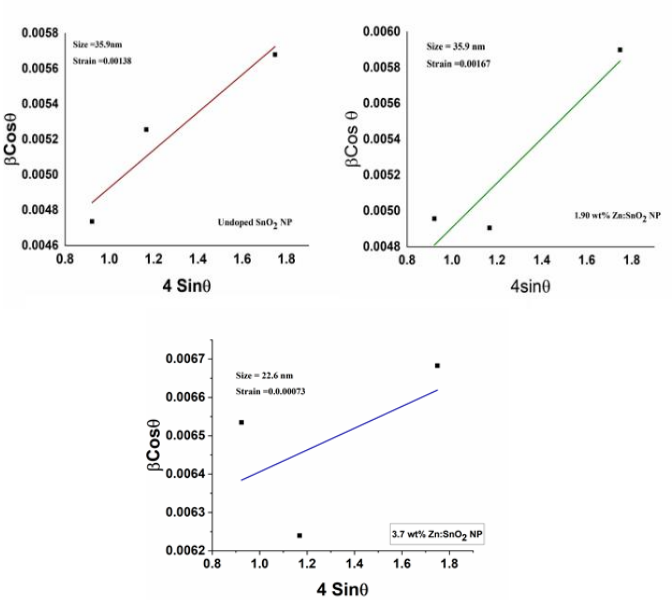

Fig. 2. Williamson- Hall plots of pristine and Zn-doped SnO_2 samples

The structural parameters are calculated from XRD data and W-H plot (Fig. 2) and is given in Table I.

TABLE I: Structural Parameters Calculated from XRD

Sample Name	SnO_2 NP		1.9 wt% Zn:SnO_2 NP		3.7 wt% Zn:SnO_2 NP	
	Scherrer Equation	W-H Plot	Scherrer Equation	W-H Plot	Scherrer Equation	W-H Plot
Grain Size(nm)	28.2	35.9	28.03	35.9	22.56	22.6
Lattice Strain	0.00429	0.00138	0.00431	0.00167	0.00541	0.00073
Stacking Fault	0.00244		0.00246		0.00305	
Dislocation Density (x10^15)	1.278		1.296		1.962	
Lattice Parameters (Å)	a=b=4.7246 Aº, c= 3.1804Aº		a=b= 4.7261 Aº, c= 3.1807Aº		a=b= 4.7168Aº, c= 3.1768Aº	

The texture coefficient of the prepared samples along the prominent planes (110), (101) and (211) is calculated using equation 2 and a graph was plotted with texture coefficient versus prominent plane (Fig. 3).

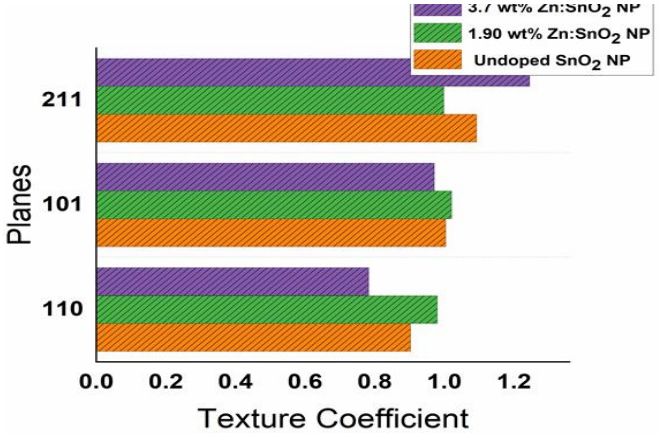

Fig. 3. Texture Coefficient of different planes.

The equation for the texture coefficient for specific plane (hkl) is given by

$$TC_{(hkl)} = \frac{\frac{I(hkl)}{I_0(hkl)}}{\frac{1}{n}\sum_1^n \frac{I(hkl)_i}{I_0(hkl)_i}} \quad \text{..... (2)}$$

Where, $TC_{(hkl)}$ is the texture coefficient of the (hkl) plane.

I (hkl) is the measured intensity of the (hkl) plane from the XRD pattern and $I_0(hkl)$ is the standard intensity of the (hkl) plane from a reference pattern and n is the number of diffraction peaks considered.

B. Morphological analysis

Fig. 4 shows the FESEM images of pristine and Zn doped Tin oxide Nanoparticles annealed at 500 °C. There is a significant agglomeration of particles in all samples, which is common in nanoparticle synthesis In Fig. 4(a) the individual particles are not distinctly visible, and this indicates that the pristine tin oxide has a high degree of aggregation.

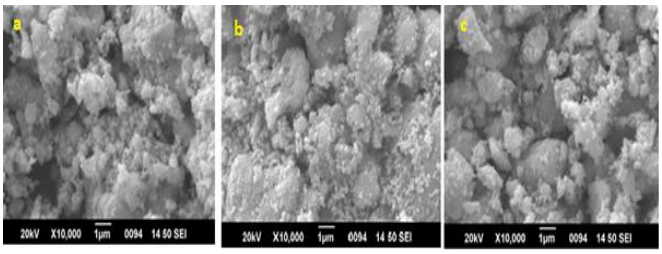

Fig.4.SEM Micrographs of (a) Pristine , (b)1.9 wt% Zn doped SnO_2 NP (c) 3.7 wt% Zn doped SnO_2 NP

In 1.9wt.% Zn-doped SnO_2 NP, the agglomeration seems to persist but the particle size may be slightly reduced. There is a potential refinement in the particle size and a slight change in the morphology for 3.7 wt.% Zn doped SnO_2 NP. Thus, Zn doping facilitates the reduction in particle size, as in Fig. 4(c). This may be attributed to the increase in surface area of the Zn-doped nanoparticles [11].

C. Optical Studies

Diffuse Reflectance Spectroscopy (DRS) and Tauc plots were employed to determine the optical band gap of the nanoparticles. Fig. 5 presents the DRS spectra of pristine SnO_2, 1.9 wt% Zn-doped SnO_2, and 3.7 wt% Zn-doped SnO_2. The calculated band gap energies range from 3.22 eV to 3.10 eV.

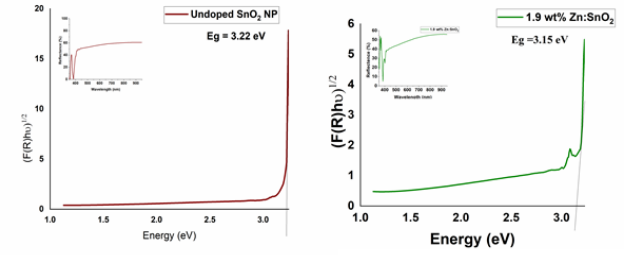

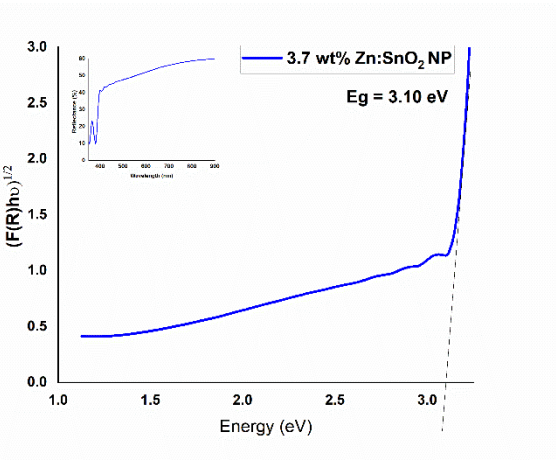

Fig. 5. Diffused Reflectance Spectroscopy- Tau plots of a) Pristine (b)1.9 wt% Zn doped SnO2 NP (c) 3.7 wt% Zn doped SnO_2 NP

Zn doping is known to introduce defects, such as oxygen vacancies or interstitial zinc atoms, which generate localized states within the band gap. These defect states serve as intermediate energy levels, reducing the energy required for electronic transitions, thereby lowering the overall band gap [12], [13].

D. FTIR

In Fig. 6 Fourier Transform Infrared Spectrum (FTIR) of Pristine and Zn-doped Tin oxide Nanoparticles are plotted. The peaks at 459 cm^{-1} and 604 cm^{-1} are generally due to Sn-O stretching vibrations in Tin oxide. This confirms, the materials core structure of Tin oxide. The peak at 924 cm^{-1} indicates the vibrations associated with Zn-O bonds. Changes in these regions are due to the doping with Zinc and are visible in the FTIR spectrum compared to pristine tin oxide nanoparticle.

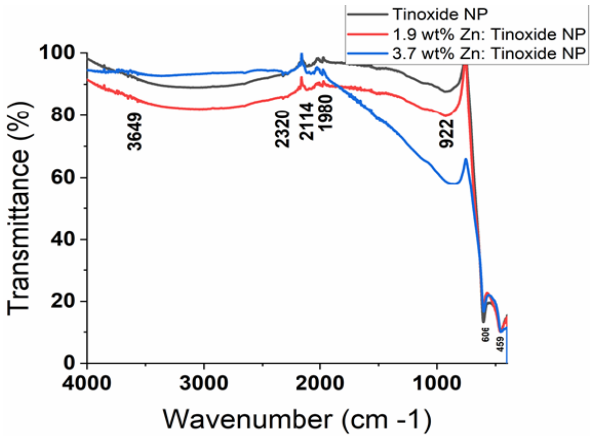

Fig. 6. Fourier Transform Infrared Spectrum of Pristine ,1.9 wt% Zn doped SnO2 NP and 3.7 wt% Zn doped SnO_2 NP

The peaks at 1976 cm^{-1} and 2117 cm^{-1} are due to metal oxide lattice vibrations and may be linked with the changes introduced by doping with Zinc, whereas the peak at 3651 cm^{-1} is attributed due to O-H stretching vibrations from the surface of hydroxyl groups or adsorbed water molecules on the nanoparticles. It is common in materials having surface interaction with atmospheric moisture. The shifts and

intensity changes in the FTIR spectra suggest the structural and bonding modifications in the doped samples [14].

Additionally, the intensity variations and shifts in these peaks with Zn doping suggest significant modifications in the local environment of the metal-oxygen bonds [15]. These modifications may arise from the substitution of Zn^{2+} for Sn^{2+}, introducing oxygen vacancies and altering the overall bonding configuration [16], [17]. The observed changes in the FTIR spectra provide further evidence of the structural and chemical alterations in the doped SnO_2 nanoparticles, likely affecting their surface properties and interaction with external species, which can be crucial for applications such as gas sensing [18].

IV. CONCLUSION

The pristine and Zn-doped SnO_2 nanoparticles were successfully synthesized via the co-precipitation method and annealed at 500°C. XRD analysis confirmed the polycrystalline nature of the samples, with a significant reduction in crystallite size observed for the 3.7 wt% Zn-doped SnO_2 nanoparticles. The crystallite size reduction was further validated using Williamson-Hall plots and supported by FESEM imaging. A decrease in peak intensity was noted in the XRD pattern, particularly for preferred orientations at higher Zinc dopant concentrations. Additionally, the band gap energy of the Zn-doped samples decreased at this dopant level, likely due to an increase in carrier concentration. FTIR spectroscopy confirmed the formation of SnO_2 nanoparticles, with observed shifts and intensity changes in the spectra of the 3.7 wt% Zn-doped sample suggesting significant structural alterations. These findings, particularly the reduced grain size and modified spectral characteristics, highlight the potential of Zn-doped SnO_2 nanoparticles for gas sensing applications.

ACKNOWLEDGMENT

The author (AJ) gratefully acknowledges the financial assistance from FISAT, Angamaly (letter No. 07/SMR/2023-24/FISAT) and the research seed grant (No. KTU/RESEARCH 3/1082/2022 dated 26/02/2023) from KTU. The authors thank the management of Mar Athanasius College, Kothamangalam, and FISAT, Angamaly, for providing the facility to do the research work and also acknowledge STIC, CUSAT for XRD, SEM, DRS and FTIR analysis.

REFERENCES

[1] Sarkar S, Guibal E, Quignard F, SenGupta AK. Polymer-supported metals and metal oxide nanoparticles: synthesis, characterization, and applications. Journal of Nanoparticle Research. 2012 Feb; 14:1-24.

[2] Sagadevan S, Lett JA, Fatimah I, Lokanathan Y, Léonard E, Oh WC, Hossain MM, Johan MR. Current trends in the green syntheses of tin oxide nanoparticles and their biomedical applications. Materials Research Express. 2021 Aug 13;8(8):082001.

[3] Nayral C, Viala E, Fau P, Senocq F, Jumas JC, Maisonnat A, Chaudret B. Synthesis of tin and tin oxide nanoparticles of low size dispersity for application in gas sensing. Chemistry–A European Journal. 2000 Nov 17;6(22):4082-90.

[4] Sagadevan S, Johan M, Bin R, Aziz FA, Hsu HL, Selvin R, Hegazy HH, Umar A, Algarni H, Roselin SL. Influence of Mn doping on the properties of Tin oxide nanoparticles prepared by Co-precipitation method. Journal of Nanoelectronics and Optoelectronics. 2019 Apr 1;14(4):583-92.

[5] Sujatha K, Seethalakshmi T, Shanmugasundaram OL. Synthesis, characterization of nano tin oxide via co-precipitation method. Nanotechnology Research and Practice. 2016(3):98-105.

[6] Sivakumar S, Manikandan E. Enhanced structural, optical, electrochemical and magnetic behavior on manganese doped tin oxide nanoparticles via chemical precipitation method. Journal of Materials Science: Materials in Electronics. 2019 Apr 1; 30:7606-1

[7] Tazikeh S, Akbari A, Talebi A, Talebi E. Synthesis and characterization of tin oxide nanoparticles via the Co-precipitation method. Materials Science-Poland. 2014 Jan; 32:98-101

[8] Senthilkumar V, Senthil K, Vickraman P. Microstructural, electrical and optical properties of indium tin oxide (ITO) nanoparticles synthesized by co-precipitation method. Materials Research Bulletin. 2012 Apr 1;47(4):1051-6.

[9] Shahzad N, Ali N, Shahid A, Khan S, Alrobei H. Synthesis of Tin xide Nanoparticles in order to study its properties. Digest Journal of Nanomaterials & Biostructures (DJNB). 2021 Jan 1;16(1).

[10] Altaf U, Ansari MZ, Rubab S. Influence of aluminium doping on structural and optical properties of tin oxide nanoparticles. Materials Chemistry and Physics. 2023 Mar 1; 297:127304.

[11] Vidhya M, Archana R, Sadayandi K, Suresh S, Gunasekaran S, Podder J, Mohammad F, Al-Lohedan HA, Oh WC. Comparison of sunlight-driven photocatalytic activity of semiconductor metal oxides of tin oxide and cadmium oxide nanoparticles. Optik. 2020 Sep 1; 217:164878.

[12] Din SU, Kiani SH, Haq S, Ahmad P, Khandaker MU, Faruque MR, Idris AM, Sayyed MI. Bio-synthesized tin oxide nanoparticles: Structural, optical, and biological studies. Crystals. 2022 Apr 26; 12(5):614.

[13] Koppala S, Balan R, Banerjee I, Li K, Xu L, Liu H, Kumar DK, Reddy KR, Sadhu V. Room temperature synthesis of novel worm like tin oxide nanoparticles for photocatalytic degradation of organic pollutants. Materials Science for Energy Technologies. 2021 Jan 1; 4:113-8.

[14] Senthilkumar V, Vickraman P, Ravikumar R. Synthesis of fluorine doped tin oxide nanoparticles by sol–gel technique and their characterization. Journal of Sol-Gel Science and Technology. 2010 Feb; 53:316-21.

[15] Tazikeh S, Akbari A, Talebi A, Talebi E. Synthesis and characterization of tin oxide nanoparticles via the Co-precipitation method. Materials Science-Poland. 2014 Jan; 32:98-101.

[16] Krishnakumar T, Jayaprakash R, Pinna N, Phani AR, Passacantando M, Santucci S. Structural, optical and electrical characterization of antimony-substituted tin oxide nanoparticles. Journal of Physics and Chemistry of Solids. 2009 Jun 1; 70(6):993-9.

[17] Krishnakumar T, Pinna N, Kumari KP, Perumal K, Jayaprakash R. Microwave-assisted synthesis and characterization of tin oxide nanoparticles. Materials letters. 2008 Jul 15; 62(19):3437-40.

[18] Gilstrap RA, Capozzi CJ, Carson CG, Gerhardt RA, Summers CJ. Synthesis of a nonagglomerated indium tin oxide nanoparticle dispersion. Adv. Mater. 2008 Nov 3; 20(21):4163-6.